Growth and Structure of the First Layers of Ice on Ru(0001) and Pt(111)

Sabine Maier,[1,2] Barbara A. J. Lechner,[1] and Miquel Salmeron*[,1,3]

[1]Materials Sciences Division, Lawrence Berkeley National Laboratory, Berkeley, CA 94709, USA

[2]Department of Physics, Friedrich-Alexander University of Erlangen-Nürnberg, Erwin-Rommel-Strasse 1, 91058 Erlangen, Germany

[3]Department of Materials Science and Engineering, University of California, Berkeley, CA 94720, USA

KEYWORDS: Scanning tunneling microscopy, ice growth, hydrogen-bonding, water

ABSTRACT: Scanning tunneling microscopy was used to probe the structure and growth of the first few layers of water on Ru(0001) and Pt(111) at the molecular level. The surface-bound first layer is composed of a mixture of water molecules forming hexagonal structures, both in registry and out-of-registry with the substrate atoms. The hexagons are connected by pentagonal and heptagonal units. At temperatures below 140 K, this layer structure gives rise to the growth of metastable amorphous structures in the second and higher layers. We found that in the transition from amorphous to crystalline ice the structure of the original bottom layer changes to one in perfect local registry with the hexagonal surfaces of Ru(0001) and Pt(111). We further discovered structural defects in the form of extended one-dimensional lines of five- and eight-membered rings that are domain boundaries and stacking faults in the growing ice layers, which lead to the formation of metastable cubic ice.

Introduction

The interaction of water and ice with solid surfaces influences a wide variety of phenomena in nature, science and technology.[1] Since the physical and chemical processes at the ice-solid interface depend on the molecular arrangement of the molecules, a large effort is underway to understand these interfaces using a variety of techniques and theoretical methods. Low temperature scanning tunneling microscopy (STM) in combination with density functional theory has become a powerful tool to help reach that goal,[2-5] although the majority of studies so far have been devoted to studying single water layers deposited on hexagonal single crystal metal surfaces. The studies have shown that water grows initially epitaxially conforming to the surface forming a H-bonded hexamer network. However, due to the 2-dimensional topological constraint, fully H-bonded structures cannot form and the growing layer must accommodate an increasing number of dangling H-bonds, from 1 on each hexagonal ring to 3 for extended islands.[6] On several metals, the comparable energy of the H-bond and the O-metal bond strengths, together with the mismatch between ice and substrate lattices lead to the formation of distorted structures relative to the conventional ice-like arrangement. For example, on Pd(111), Pt(111) and Ru(0001) the first water layer features bonding-motifs of rotated hexagonal rings bridged by pentagonal and heptagonal rings.[7-9] A characteristic of these surfaces is that the dangling OH bonds of the water monolayer do not stick out into the vacuum (H-up), because the H-down configuration maximizes interaction with the underlying metal substrate.[10-12] Therefore, the first layer is expected to rearrange for ice nucleation to form multilayers with hexagonal structure. So far however, most studies have been limited to the first layer, and a molecular picture of the hydrogen-bonding structures of water multilayers has remained elusive so far.

From electron diffraction and spectroscopic experiments it is commonly accepted that ice films grow amorphous below 120 K and crystalline at higher temperatures on close-packed metal surfaces.[3,13-17] In recent STM measurements on Pt(111), a competing nucleation of hexagonal and cubic ice has been observed and analyzed based on island shapes and dislocations.[18-22] In these studies the molecular-level structure of the ice clusters was not resolved, and yet this information is key to deciphering the binding geometry of the ice film to the substrate and the proton ordering.[23,24] It is also crucial to understand the structure of defects and dislocations that distort the ideal hydrogen-bonding networks. The hydrophobic Cu(111) is the only surface, to our knowledge, where molecularly resolved STM experiments of crystalline water multilayer

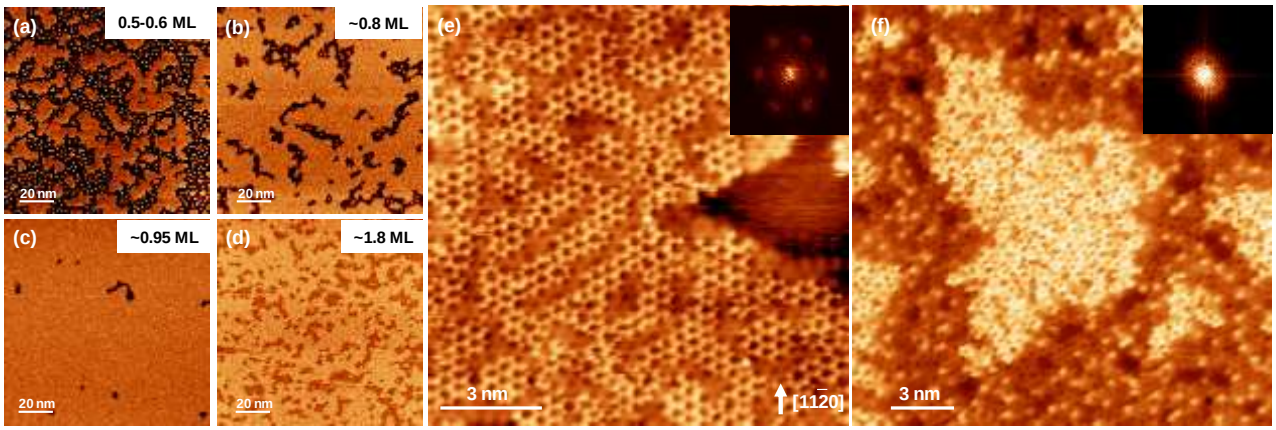

Figure 1. Growth and structure of amorphous ice on Ru(0001) at 140K. (a)-(d) STM image sequence of the formation of a first and second water layer. The darker area corresponds to exposed Ru, while lighter colors correspond to first and second layers. The apparent height of the first layer is 80-160 pm and the second layer around 70 pm. (e) Molecularly resolved STM image of the first water layer showing low lying (darker, in registry with the substrate) and high lying (brighter, rotated by 30°) hexamers connected by pentagons and heptagons. Inset: FFT of the image, the spots are due to the high lying hexamers. A region of bare Ru substrate is visible on the right side. (f) First layer water with patches of amorphous second layer (brighter). The FFT from the second layer region (inset), shows no pronounced peaks. STM parameters: 77 K, (a) 311 mV, 10.9 pA, (b) -320 mV, 10.5 pA, (c) -155 mV, 4.4 pA, (d) -382 mV, 2.3 pA, (e) 175 mV, 10.9 pA, (f) -379 mV, 3.2 pA.

clusters are available.[25] A variety of complex water structures are formed on Cu(111) during the crystallization to hexagonal and cubic ice; however, in none of them a I_h(0001) or I_c(111) bilayer termination was found.

Here, we present new molecularly resolved STM measurements showing the molecular structure of amorphous and crystalline ice grown on Ru(0001) and on Pt(111). We discuss how the first layer has to rearrange from pentagons, hexagons and heptagons into a purely hexagonal ice-like structure in order to facilitate crystalline ice growth. Further, we introduce a new hydrogen-bonding motif consisting of extended one-dimensional defects of five- and eight-membered rings, due to stacking faults and ice crystal grain boundaries.

Experimental Methods

The adsorption of water was studied in ultra-high vacuum using a home-built low-temperature STM,[26] with a separate preparation chamber. All the experiments were recorded in constant-current mode at liquid nitrogen (77 K) or liquid helium temperature (5 K). Images were taken using tunneling conditions with bias voltages below 450 mV, the energy of the O-H stretch mode, and low currents to ensure the water structures are not changed by tip-induced restructuring or dissociation.[27] The Ru(0001) crystal was initially cleaned by cycles of argon ion sputtering at 1 keV, and annealing at 1600 K. Further, annealing and cooling cycles between 770 K and 1770 K in a partial oxygen atmosphere (2×10^{-8} Torr) were performed in order to deplete the subsurface layers from carbon impurities. The Pt(111) crystal was cleaned by argon ion sputtering at 1 keV and annealing to 1300 K, followed by heating in 4×10^{-7} Torr oxygen at 1200 K for 15 min to remove carbon contaminations. A final annealing step to 1200 K in UHV removed residual oxygen from the surface. Both surfaces were characterized by STM to determine the nature and concentration of pre-adsorbed species on the sample (mainly O and C, with a total coverage of less than 1%). We used ultrapure water (deuterium-depleted ≤1 ppm D_2O, Sigma Aldrich), additionally cleaned by freeze-pump-thaw cycles. The water was leaked through a capillary tube pointing to the sample held at 140-145 K. In the case of Pt(111), deposition was also performed at 5 K followed by annealing to 140 K. The deposition rate was 0.4–0.6 ML/min. The indicated water coverages refer to fractions of the saturation coverage of a water monolayer (ML) on the close-packed metal surface.

Results and Discussion

1. Growth and Structure of Amorphous Ice Layers

The STM images in Fig. 1 (a)-(d) show the growth and morphology of water layers deposited on Ru(0001) at 140 K. At this temperature and below, the growth proceeds layer by layer. The molecular structure of the first layer consists of hexagonal water rings with two types of orientation. One is in registry with the hexagonal metal surface and covalently bonded through the oxygen atoms, the other is rotated by 30° and slightly lifted off the substrate. The two are connected by pentagonal and heptagonal rings.[9] The Fast Fourier Transform (FFT) of the first layer shows a hexagonal symmetry originating from the locally ordered rotated hexamers. When additional water monomers adsorb on top of the first layer they bind most often to the lifted molecules (see Fig. S1)

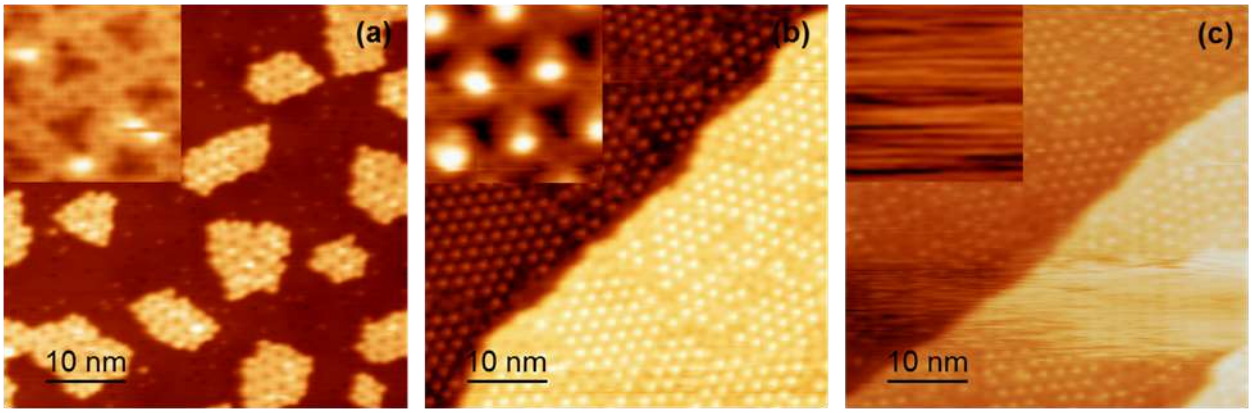

Figure 2. Ice growth on Pt(111) at 140 K. (a) At coverages below 1 ML water forms islands with *(√37x√37)-R25.3°* structure (bright patches) on Pt(111). (b) Upon increasing the coverage, the layer adopts a *(√39x√39)-R16.1°* structure that covers the surface completely, here shown across an atomic step in the Pt(111) substrate. The brighter spots are due to single second layer molecules forming a periodic array on top of the √39 structure. (c) Further growth results in disordered second layer islands that are mobile under the tip. Magnified views of the sub-ML, complete first layer and second layer islands, respectively are shown in 5 nm x 5 nm insets. STM parameters: (a) 150 mV, 13.5 pA, 5 K, (b) 210 mV, 14.5 pA, 5 K, (c) 210 mV, 14.4 pA, 5 K.

The image in Fig. 1(f) shows a large second layer patch containing randomly distributed 5-, 6-, and 7-membered rings (see also Fig. S2). An FFT analysis of this second layer (see inset) confirms its amorphous nature. The amorphous structure indicates that the crystallization of water is kinetically hindered below 140 K on Ru(0001), in agreement with results obtained by ensemble-averaging techniques.[13,28]

Similar behavior is also observed for ice growth on Pt(111), as shown in Fig. 2. At coverages slightly below a full monolayer, water forms a *(√37 x √37)-R25.3°* structure (Fig. 2(a)) consisting of a mixture of flat lying hexamers in registry with the Pt substrate (darker region of the unit cell), and rotated high-lying hexamers forming the brighter triangles. Like on Ru, the two types of hexamers are connected by pentagonal and heptagonal rings. At a slightly higher coverage a different structure with *(√39 x √39)-R16.1°* periodicity is formed (Fig. 2(b)). This structure has a similar arrangement of low lying hexamers (dark contrast in the image) in registry with the Pt substrate, and rotated, high lying hexamers (brighter). The two are again connected by pentagonal and heptagonal rings. This denser structure often includes an additional top molecule per unit cell, visible as a regular array of bright protrusions in the image. These structures agree with previous STM experiments.[7,8] In contrast to the case of Ru(0001), the first water layer on Pt(111) exhibits long-range order. It is interesting to notice that the second layer molecules in the *√39* structure expose a dangling OH group, as was shown by infrared spectroscopy[10].

Further deposition of water results in the formation of disordered second layer islands, seen in the bottom half of Fig. 2c. In contrast to the amorphous water layers on Ru(0001), we could not resolve the second layer in the STM images as the molecules are too mobile even at 5 K, likely due to strong interactions with the STM tip, resulting in the streaks observed along the scan direction (horizontal in Fig. 2(c)).

2. Transformation from Amorphous to Crystalline Ice

It has been suggested that the heterogeneous first water layer containing rotated and non-rotated hexamers connected by pentamers and heptamers has to reconstruct to facilitate the growth of subsequent hexagonal or cubic crystalline layers.[21] This structural modification, not documented in previous STM studies, is the topic of this section.

Fig. 3(a) shows patches of second water layer on Ru(0001) on top of a first water layer covering most of the substrate. Although the second layer is mostly amorphous, a few ordered patches are also present, as the one shown by the framed area in Fig 3(a), magnified in (b). The ordered second layer patches have a *(√3 x √3)-R30°* structure relative to the Ru substrate, suggesting that the first layer underneath is equally ordered. We found that after repeated scanning the molecules in the second layer can be removed by the tip, exposing a perfectly ordered hexagonal network in the first layer, as shown in Fig. 3(c). The scanning was done with bias voltages < 400 meV to prevent a potential tip induced dissociation of molecules through vibrational excitations.[29] The exposed first layer hexamers are of the low-lying type, i.e., in registry with the underlying substrate. This finding strongly suggests that ordered ice-like growth requires restructuring of the original layer composed of hexagons, pentagons, and heptagons into a commensurate hexagonal structure.

Similarly, the *(√39 × √39)-R16.1°* first layer on Pt(111) is not a suitable substrate for crystalline multilayer films, as evident in the disordered island shown in Fig. 2(c). Instead, the slightly energetically less favorable[12] *(√3 × √3)-R30°* structure is suggested as the interface layer in registry with the Pt(111) surface.[21] As we show next, crystalline island growth occurs only on the *√3* water monolayer on Pt(111).[30,31]

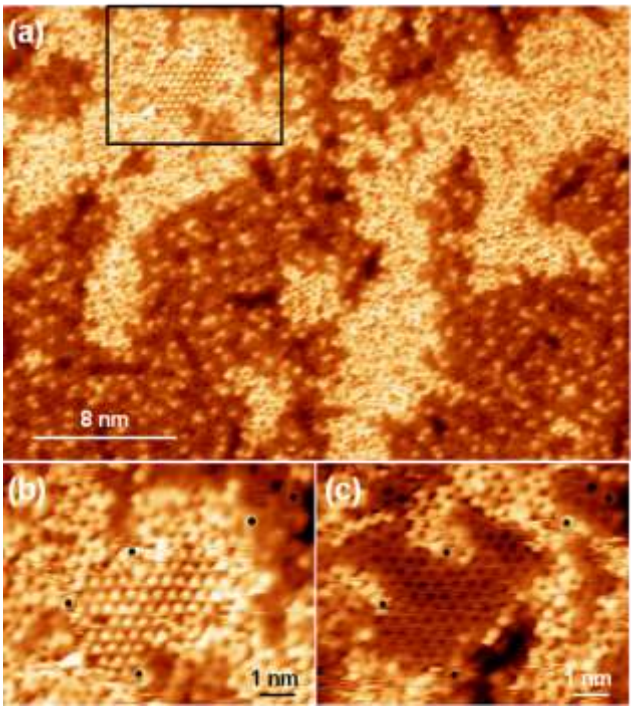

Figure 3. Amorphous second layer ice containing ordered patches on Ru(0001). (a) A complete first layer is partially covered by a second layer after depositing water at 140 K. The area in the frame, containing an ordered patch of second layer water is shown magnified in (b). (c) After repeated scanning the second layer molecules were removed, exposing a hexagonal network of first layer molecules in registry with the underlying substrate. The observation of long-range order in the exposed first layer supports the idea that ordered ice-like growth requires restructuring of the first layer. The black dots in (b) and (c) are reference points to compare identical positions. STM parameters: (a)-(c) -379 mV, 3 pA, 77 K.

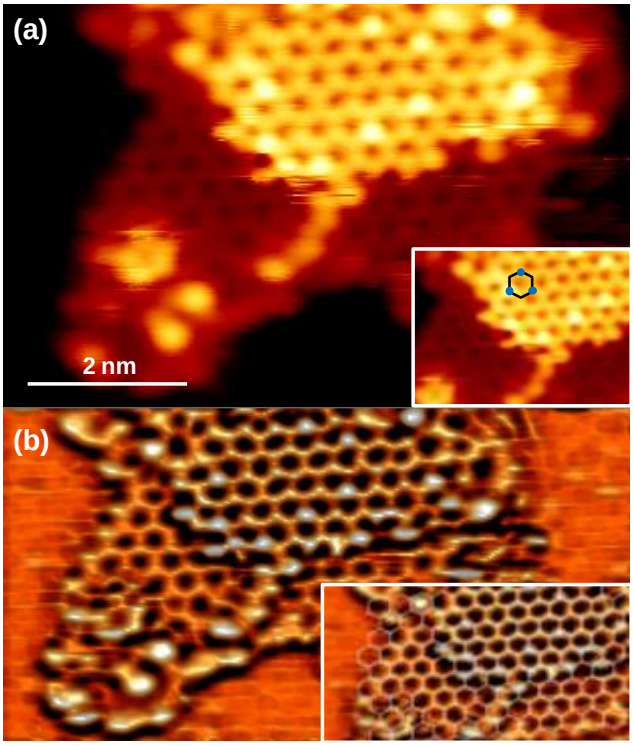

Figure 4. Atomic structure of ice-clusters on Ru(0001). (a) Molecularly resolved crystalline cluster containing two water layers surrounded by exposed Ru. The blue dots in the inset show the preferred adsorption sites of third layer molecules within a hexagon. (b) The first and second layer are in registry with the underlying substrate, with the hexagonal rings precisely stacked above each other, as shown by the Laplace and low pass filtered image in (b). STM parameters: -263 mV, 3.2 pA, 77 K.

3. Molecular Structure of Multilayer Ice Clusters

It is well established that the amorphous water grown at low temperatures crystallizes above a certain threshold around 150 K.[3,13,19] However, when the amorphous films on Ru(0001) are heated, crystallization is competing with desorption[13] and dissociation.[27,32] These effects can be minimized by depositing water at 145 K. Fig. 4 shows an STM image of the water film formed at this temperature. The image reveals areas containing extended hexagonal networks both in the first and second layer, confirming that the temperature range for the transition of amorphous to crystalline growth is a few Kelvin. The growth of crystalline multilayer islands is in agreement with previously reported rare gas desorption experiments on Ru(0001).[13] In our experiments we did not observe signs of dissociation in the form of characteristic narrow stripes.[27,32]

The high resolution STM image in Fig. 4 shows clearly the honeycomb lattice of water molecules with the first and second water layers in perfect registry with each other (see inset Fig. 4(b)). Furthermore, the orientation with respect to the substrate is the same for all domains. The measured periodicity of the honeycomb network fits well with that of the $\sqrt{3}$ structure. In Fig. 4, there is no noticeable contrast difference between individual water molecules within a hexagon, which prevents any conclusion about the proton ordering or the staggering of contiguous O atoms. However, in spite of the similar contrast the six corners are different, as revealed by the additional water molecules on top of the second layer. These molecules, with an apparent height of 35 pm, were found to always bind to the same three out of the six corners of the second layer hexamers, marked by blue dots in the Fig. 4(a) inset. This observation indicates that the hexamer has indeed a 3-fold structure. This could originate from a staggered (chair) arrangement of molecules, an alternating orientation of H bonds, or both. The symmetry of the 3-corner occupation pattern does not change as the molecules move over the surface at the imaging temperature of 77 K, as shown in Figs. S3 and S4.

A clue to the nature of the three distinct corner sites is provided by empirical and DFT calculations. Accordingly, the adsorption of ad-molecules on the basal plane surface of ice Ih is most favorable for sites with one or two dangling H atoms (DH), while sites with no DH bind only weakly and sites with three DHs do not provide stable binding.[33,34]

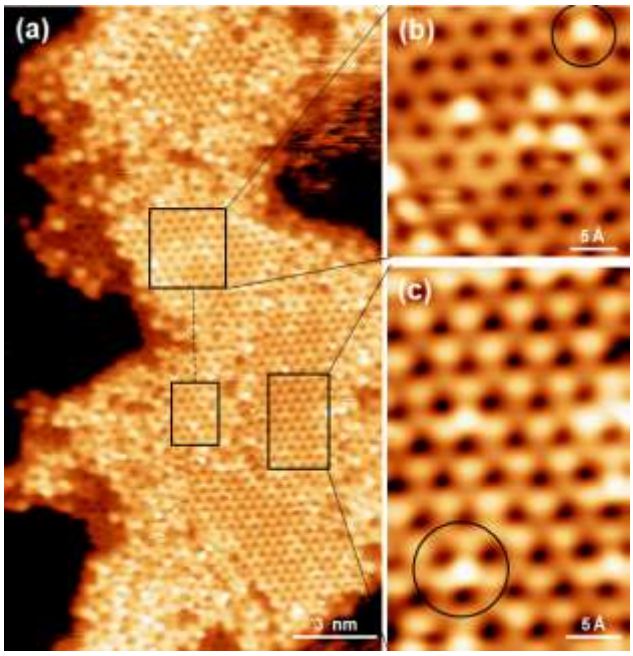

Figure 5. Structure of a two layer high ice film on Ru(0001) with additional third layer molecules. (a) STM image showing bare Ru (black), first layer (reddish) and second layer ice (brighter). The contrast in the second layer changes from being similar for all water molecules within a hexagon (regions in the top and left framed squares), shown magnified in (b), to a contrast where the apparent height alternates by around ~20 pm between neighboring water molecules, in the region magnified in (c). The circles highlight additional third layer molecules in both structures. The fact that both contrasts are present side by side in the horizontally scanned image (bottom left and right framed regions) indicates that the difference is not due to different functionalities or to a structural change in the STM tip apex. STM parameters: (a)-(c) -263 mV, 3.3 pA, 77 K.

Another manifestation of the different nature and termination of top water molecules in growing ice is the observation of a second type of STM contrast between molecules in the honeycomb networks of the second layer, as shown in Fig. 5. The first type, visible in the top and left side square frames of Fig. 5(a), shown magnified in (b), is like that in Fig. 4, with each molecule in the six hexagon corners having a similar contrast. The second type, visible in the bottom right frame, shown magnified in Fig. 5(c), is distinguished by alternating apparent heights, differing by about 20 pm between neighboring water molecules. In addition, the apparent height of third layer ad-molecules in this second structure is significantly smaller. This can be rationalized either by a different orientation or stacking of water molecules occurring in hexagonal and cubic ice structures. Alternatively, periodic ad-layer structures could explain the second contrast. However, the previously reported *(2 x 1)*,[25,35] *(2 x 2)*[25,36] and *c(2 x 4)*[25] structures do not fit the contrast observed in Fig. 5.

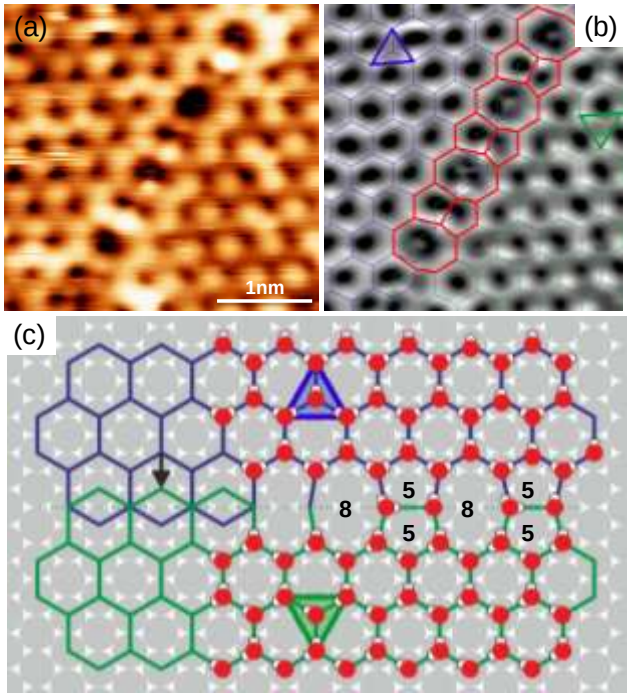

Figure 6. Atomic structure of defect lines in a two layer ice film on Ru(0001). (a) STM image showing a defect-line of five- and eight-membered ring motifs. (b) The overlaid grid on the filtered image (Laplace and low pass filtered) indicates that the honeycomb lattices on both sides of the defect are laterally shifted. The alternate orientation of the colored triangles suggests a different stacking arrangement. (c) Schematics to illustrate that the one-dimensional defects can be formed by a translation of two half-lattices relative to one another. STM parameters: -263 mV, 3.2 pA, 77 K.

Another aspect to the structure of the ice layers is provided by defects in the film. The 2-layer high ice clusters on Ru(0001) (Fig. 4) consist mainly of hexagons with a few pentagons at the periphery. In addition, molecularly resolved images often show defect lines oriented along the [1 1 -2 0]-directions (see Fig. S5). The molecules in the defect line adopt a peculiar arrangement of pairs of five-membered rings separated by eight-membered rings, as that shown in Fig. 6. We note that this is a novel bonding motif for water molecules on surfaces. Previously, five-membered rings were always reported to occur in combination with seven-membered rings instead of eight-membered rings in water layers.[2] These one-dimensional defects can be formed by a translation of two half-lattices relative to one another by one lattice constant (Fig. 6(c)). The filtered STM image with the overlaid lattice in Fig. 6(b) confirms that the observed line defects are relat-

ed to a lateral shift of the ice-honeycomb network of adjacent domains. In addition the stacking of the lattice on both sides of the defects appears different, as can be seen from the orientation of the colored triangles. Within each half-layer, three high-lying oxygen atoms surround either a lower contrast oxygen atom (colored triangle) or the core of the hexamer. The different orientation can originate from stacking faults that coincide with the formation of metastable cubic ice with respect to the Ru substrate lattice, as the orientation of these colored stacking triangles alternate from layer to layer in hexagonal ice but not in cubic ice.[22] Alternatively, it could arise from domain boundaries between two crystals that are not in registry and grow together. The latter requires the presence of the one-dimensional defects also in the interface layer. Although the first layer is mostly covered by a second layer, we observed small patches of exposed first layer. There, we also found defects with 5-8 membered rings, demonstrating that such defects can also occur in the water interface layer (Fig. S6). The defect lines provide the possibility for the relief of misfit strain between water and the metal lattice.

Similar extended one-dimensional defects with a structural motif of coupled five- and eight-membered rings have been observed in two-dimensional hexagonal materials such as graphene.[37] Such defect lines have been recently predicted in molecular dynamics (MD) calculations of stacking fault formation in unsupported bulk ice I_h along the (0001) ice plane by Pirzadeh et al.[38] However, the occurrence of such 5-8 ring defects has not been confirmed experimentally until now. MD calculations show that the planar defects facilitate the formation of stacking faults, coinciding with a change from ice I_h to the metastable cubic ice I_c.[1] The observation of predicted bulk-like properties in our STM experiment confirms the ice-like structure of the second layer water. Thürmer et al. showed the occurrence of cubic ice on Pt(111) at low temperatures in STM experiments. Their model is based on the assumption that the structural mismatches occur at the position of substrate steps, leading to formation of screw dislocations in the ice crystal.[19] Our measurements show that on Ru(0001) defect lines that facilitate the nucleation of cubic ice also occur away from step locations. The frequency of formation of such defect lines is strongly dependent on the temperature as higher temperatures would likely anneal such defects in a growing crystal. Since water dissociation occurs on Ru(0001) at only slightly higher annealing temperatures, one is limited to a temperature range below about 150 K.[39]

Fig. 7 shows STM images of crystalline first and second layer water structures on Pt(111). In contrast to the amorphous second layer islands on the *(√39 × √39)-R16.1°* ML in Fig. 2, we find that perfectly ordered crystalline islands can grow on the *(√3 × √3)-R30°* layer commensurate with the Pt lattice. This observation is in line with the finding that on Ru(0001) the first water layer needs to rearrange to facilitate the growth of ordered ice islands. While the *√3* structure is energetically less favorable (by 0.1 eV/molecule[7]) than the *√37* and *√39* structures on Pt(111),[7] we find that it can be formed by deposition at temperatures around 140 K in a residual H_2 background atmosphere.[40] The presence of a low coverage of H atoms on the surface, on the order of a few percent of a ML, is apparent in the dark centers of some of the water hexagons. A similar observation was previously made on Ru(0001), where partial dissociation of a water ML resulted in H atoms located in the center of H_2O hexagons.[32] In contrast to the *√3* ML on Pt(111) created by electron injection,[30,31] the molecules are not dissociated in the present case. Evidence for the intact nature of the water molecules lies in the fact that the water layer can be desorbed completely by annealing to 160 K, with none of the higher temperature desorption peaks arising which are characteristic for OH + H recombination.

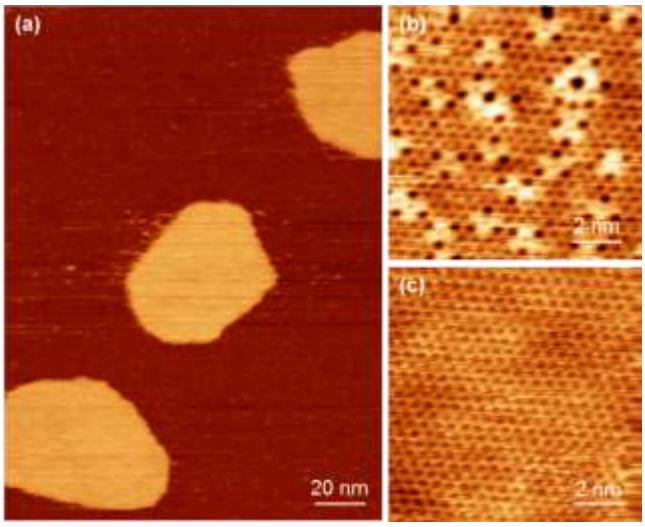

Figure 7. Crystalline water islands on a complete (√3 × √3)-R30° ML on Pt(111). (a) Image of a complete first layer with *(√3 × √3)-R30°* on Pt(111) (dark), with islands of second layer water. (b) Magnified view of the *(√3 × √3)-R30°* structure of the first water layer, exhibiting dark defects, most likely due to hydrogen atoms located in the center of the water rings.[40] (c) Flat and defect-free *(√3 × √3)-R30°* structure of the second layer islands. STM parameters: (a) 201 mV, 17.5 pA, 77 K, (b) 153 mV, 10.0 pA, 77 K, (c) -243 mV, 22.9 pA, 77 K.

The molecular-scale details in Fig. 7(b) show that the images of molecules in the *√3* layer do not have a uniform contrast. Instead the regions in the neighborhood of the H atoms (dark centers in water hexagons) appear brighter in STM. This could arise from an electronic modification of the water molecules and/or a slight lift of the molecules off the surface. In contrast, the second layer islands exhibit a small overall corrugation and have essentially a perfect *√3* arrangement, as shown in Fig. 7(c). In a previous study we observed that ammonia (NH_3) molecules can adsorb on the first *√39* and *√37* layers but only on top of the lifted water molecules which can flip their unbound H from pointing down to the metal to up into the vacuum in a rotation with zero barrier when NH_3 is nearby.[40] On

the $\sqrt{3}$ water layer, NH_3 was also observed to adsorb exclusively on the high contrast molecules, but not on the second layer islands, implying that the second layer molecules do not exhibit dangling OH groups nor flip easily to bind the ammonia molecule. Similarly, we do not observe any third layer water molecules such as those found on Ru(0001) (cf. Fig. 4) in our STM images of Pt(111). These observations are consistent with a previous study of ice growth on Pt(111) where layer-by-layer growth with all molecules either flat-lying or in a H-down orientation was found.[41] Previous investigations of the growth of water films on Pt(111) showed that amorphous ice grows layer-by-layer while crystalline growth is only observed in isolated multilayer crystallites that do not wet the monolayer.[11,18,19] However, these studies focused on the structure of thicker ice films and did not explain the transition from an incommensurate $\sqrt{39}$ ML to a hexagonal multilayer structure. Our STM experiments show that a $\sqrt{3}$ water ML that is stabilized by co-adsorption with H atoms provides a better template for a hexagonal second water layer than the $\sqrt{39}$ water layer. These findings suggest that the first water layer needs to reorder into a $\sqrt{3}$ structure to facilitate crystalline layer-by-layer growth, analogous to our findings on Ru(0001).

Conclusion

The high-resolution capability of STM to resolve the molecular structure of the first and second water layer simultaneously provides valuable details of the structure and growth mechanism of ice-like water layers on close-packed metal surfaces beyond the interface layer. First, high resolution STM images on Ru(0001) and Pt(111) revealed that the first layer, composed of 5-6-7-membered rings and rotated hexagons, has to rearrange into an ice-like layer with a $(\sqrt{3} \times \sqrt{3})$-$R30°$ structure in order to facilitate the crystalline multilayer adsorption. This indicates a clear change in the balance of interaction forces from optimizing molecule-surface interactions in the 5-6-7-ring layer to intermolecular hydrogen-bonds in the ice-like structures. Second, we observed a different growth mode of the $(\sqrt{3} \times \sqrt{3})$-$R30°$ water interface layer upon multilayer adsorption on Ru(0001) and Pt(111). While on Ru(0001) the ice-like water clusters grow in a three-dimensional way exposing the bare metal surface, on Pt(111) the interface layer wets the surface before the second layer forms. Third, we have identified a new structural motif consisting of planar defect lines on the second layer of ice-like clusters on Ru(0001). It consists of connected pairs of five-membered rings alternating with eight-membered rings bridging the boundaries between adjacent domains, which can lead to the formation of metastable cubic ice. Our STM results provide the first direct view on the atomic-level structure of water layers beyond the interface layer and ice surfaces, respectively, at low temperatures.

ASSOCIATED CONTENT

Supporting Information. Additional scanning tunneling microscopy data is presented. This material is available free of charge via the Internet at http://pubs.acs.org.

AUTHOR INFORMATION

Corresponding Author

*email: mbsalmeron@lbl.gov.

ACKNOWLEDGMENT

This work was supported by the Director, Office of Energy Research, Office of Basic Energy Sciences, Materials Science and Engineering Division, of the U.S. Department of Energy under Contract No. DE-AC02-05CH11231.

REFERENCES

(1) Petrenko, V. K.; Whitworth, R. W. *Physics of ice*; Oxford University Press, 2002.
(2) Carrasco, J.; Hodgson, A.; Michaelides, A. *Nat. Mater.* **2012**, *11*, 667.
(3) Hodgson, A.; Haq, S. *Surf. Sci. Rep.* **2009**, *64*, 381.
(4) Maier, S.; Salmeron, M. *Acc. Chem. Res.* **2015**, *48*, 2783.
(5) Feibelman, P. J. *Physics Today* **2010**, *63*, 34.
(6) Tatarkhanov, M.; Ogletree, D. F.; Rose, F.; Mitsui, T.; Fomin, E.; Maier, S.; Rose, M.; Cerdá, J. I.; Salmeron, M. *J. Am. Chem. Soc.* **2009**, *131*, 18425.
(7) Nie, S.; Feibelman, P. J.; Bartelt, N. C.; Thürmer, K. *Phys. Rev. Lett.* **2010**, *105*, 026102.
(8) Standop, S.; Redinger, A.; Morgenstern, M.; Michely, T.; Busse, C. *Phys. Rev. B* **2010**, *82*, 161412.
(9) Maier, S.; Stass, I.; Mitsui, T.; Feibelman, P. J.; Thürmer, K.; Salmeron, M. *Phys. Rev. B* **2012**, *85*, 155434.
(10) Kimmel, G. A.; Zubkov, T.; Smith, R. S.; Petrik, N. G.; Kay, B. D. *J. Chem. Phys.* **2014**, *141*, 18C515.
(11) Kimmel, G. A.; Petrik, N. G.; Dohnalek, Z.; Kay, B. D. *Phys. Rev. Lett.* **2005**, *95*, 166102.
(12) Meng, S.; Wang, E. G.; Gao, S. W. *Phys. Rev. B* **2004**, *69*, 195404.
(13) Haq, S.; Hodgson, A. *J. Phys. Chem. C* **2007**, *111*, 5946.
(14) Kondo, T.; Mae, S.; Kato, H. S.; Kawai, M. *Surf. Sci.* **2006**, *600*, 3570.
(15) Kondo, T.; Kato, H. S.; Bonn, M.; Kawai, M. *J. Chem. Phys.* **2007**, *127*, 094703.
(16) Denzler, D. N.; Hess, C.; Dudek, R.; Wagner, S.; Frischkorn, C.; Wolf, M.; Ertl, G. *Chem. Phys. Lett.* **2003**, *376*, 618.
(17) Zimbitas, G.; Haq, S.; Hodgson, A. *J. Chem. Phys.* **2005**, *123*, 174701.
(18) Thürmer, K.; Bartelt, N. C. *Phys. Rev. Lett.* **2008**, *100*, 186101.
(19) Thürmer, K.; Bartelt, N. C. *Phys. Rev. B* **2008**, *77*, 195425.
(20) Nie, S.; Bartelt, N. C.; Thürmer, K. *Phys. Rev. Lett.* **2009**, *102*, 136101.
(21) Nie, S.; Bartelt, N. C.; Thürmer, K. *Phys. Rev. B* **2011**, *84*, 035420.
(22) Thürmer, K.; Nie, S. *Proceedings of the National Academy of Sciences* **2013**, *110*, 11757.
(23) Pan, D.; Liu, L.-M.; Tribello, G. A.; Slater, B.; Michaelides, A.; Wang, E. *Phys. Rev. Lett.* **2008**, *101*, 155703.
(24) Buch, V.; Groenzin, H.; Li, I.; Shultz, M. J.; Tosatti, E. *Proceedings of the National Academy of Sciences* **2008**, *105*, 5969.
(25) Mehlhorn, M.; Morgenstern, K. *Phys. Rev. Lett.* **2007**, *99*, 246101.

(26) Shimizu, T. K.; Mugarza, A.; Cerda, J. I.; Heyde, M.; Qi, Y. B.; Schwarz, U. D.; Ogletree, D. F.; Salmeron, M. *J. Phys. Chem. C* **2008**, *112*, 7445.
(27) Tatarkhanov, M.; Fomin, E.; Salmeron, M.; Andersson, K.; Ogasawara, H.; Pettersson, L. G. M.; Nilsson, A.; Cerda, J. I. *J. Chem. Phys.* **2008**, *129*, 154109.
(28) Kondo, T.; Kato, H. S.; Bonn, M.; Kawai, M. *J. Chem. Phys.* **2007**, *126*, 181103.
(29) Mugarza, A.; Shimizu, T. K.; Ogletree, D. F.; Salmeron, M. *Surf. Sci.* **2009**, *603*, 2030.
(30) Harnett, J.; Haq, S.; Hodgson, A. *Surf. Sci.* **2003**, *528*, 15.
(31) Standop, S.; Morgenstern, M.; Michely, T.; Busse, C. *J. Phys.: Condens. Matter* **2012**, *24*, 124103.
(32) Maier, S.; Stass, I.; Cerdá, J. I.; Salmeron, M. *Phys. Rev. Lett.* **2014**, *112*, 126101.
(33) Batista, E. R.; Jónsson, H. *Computational Materials Science* **2001**, *20*, 325.
(34) Thierfelder, C.; Hermann, A.; Schwerdtfeger, P.; Schmidt, W. G. *Phys. Rev. B* **2006**, *74*, 045422.
(35) Nordlund, D.; Ogasawara, H.; Wernet, P.; Nyberg, M.; Odelius, M.; Pettersson, L. G. M.; Nilsson, A. *Chem. Phys. Lett.* **2004**, *395*, 161.
(36) Glebov, A.; Graham, A. P.; Menzel, A.; Toennies, J. P.; Senet, P. *J. Chem. Phys.* **2000**, *112*, 11011.
(37) Lahiri, J.; Lin, Y.; Bozkurt, P.; Oleynik, I. I.; Batzill, M. *Nat Nano* **2010**, *5*, 326.
(38) Pirzadeh, P.; Kusalik, P. G. *J. Am. Chem. Soc.* **2011**, *133*, 704.
(39) Feibelman, P. J. *Science* **2002**, *295*, 99.
(40) Lechner, B. A. J.; Kim, Y.; Feibelman, P. J.; Henkelman, G.; Kang, H.; Salmeron, M. *J. Phys. Chem. C* **2015**, *119*, 23052.
(41) Su, X.; Lianos, L.; Shen, Y. R.; Somorjai, G. A. *Phys. Rev. Lett.* **1998**, *80*, 1533.

SYNOPSIS TOC